Study on 2-D Crustal Shear Wave Splitting Tomography along The Sunda-Banda Arc Transition Zone

Syuhada Syuhada[1,2],Nugroho D. Hananto[3], Chalid I. Abdullah[4], Nanang T. Puspito[5], Tedi Yudistira[5]and Titi Anggono[1]

[1]Research Centre for Physics - Indonesian Institute of Sciences (LIPI), Tangerang, Indonesia
[2]Graduate Research on Earthquake and Active Tectonics (GREAT), Institut Teknologi Bandung, Indonesia
[3]Research Centre for Geotechnology-LIPI, Bandung, Indonesia
[4]Faculty of Earth Sciences and Technology, Institut Teknologi Bandung, Indonesia
[5]Global Geophysics Research Group, Faculty of Mining and Petroleum Engineering, Institut Teknologi Bandung, Indonesia

E-mail: hadda9@gmail.com

Abstract. The Sunda-Banda Arc transition zone is an active region characterized by a change in tectonic regime from subduction of Indo-Australia oceanic lithosphere along the eastern part of Sunda Arc to collision of the Australian continental crust with islands arc in the western part of the Banda Arc. This complicated tectonic setting causes this area is an ideal place to study the crustal deformation along the plate boundary. The density contrast between the Australian continental crust and Indo-Australia oceanic crust in the transition zone may cause large stresses around the boundary between them. These plate boundary forces may control the distribution pattern of the deformation in the subduction to collision transition zone. The geometry of this deformation can be investigated using shear wave splitting (seismic anisotropy) study. We conduct shear wave splitting measurements from local earthquakes recorded at 17 broadband seismic stations around the Sunda-Banda arc transition zone. The 2-D delay time tomography is then applied to determine the first order approximation of lateral varying anisotropic layers due to the local effect of geological structures. We observe strong anisotropy regions which coincide with the geological features as possible causes of anisotropy in the Sunda-Banda Arc transition zone. For instance, the high anisotropy zone found in Timor Island can be related to the alignment of metamorphic and igneous rocks, whereas the high anisotropy area around Sumba Island might correspond to the interaction of Sumba basement with the Australian margin increasing the frictional strength at the plate boundary.

1. Introduction

The evidence of seismic anisotropy in the crust has been investigated through shear wave splitting analysis providing information on the deformation related to the regional geodynamic processes. The shear wave splitting analysis determines the fast direction of the split S waves (ϕ) and delay time between the split S waves (δt). There are two mechanisms responsible for crustal anisotropy: stress induced anisotropy and structural anisotropy [1, 2]. The previous study of shear wave splitting from local event has been conducted in the collision domain of Sunda-Banda transition zone [3]. This study observed that the crustal anisotropy in this area is not only governed by stress induced anisotropy, but

also by structure-controlled anisotropy. In this report we extend our data set using 17 GEOFONE-IA broadband three component seismometers covering two different tectonic domains, subduction and collision. We use ISC database to search shallow events (< 30 km) in the study area recorded between 2008 and 2015. We also utilize the automated shear wave splitting (MFAST) developed by Savage *et al.* [4] to estimate anisotropy parameters. We employ two-dimensional tomography method of Johnson *et al.* [5] to analyze spatial anisotropy distribution in the region. The result of this research will be used to map and to identify regions with high and low degree anisotropy that might be correlated to the possible causes of anisotropy.

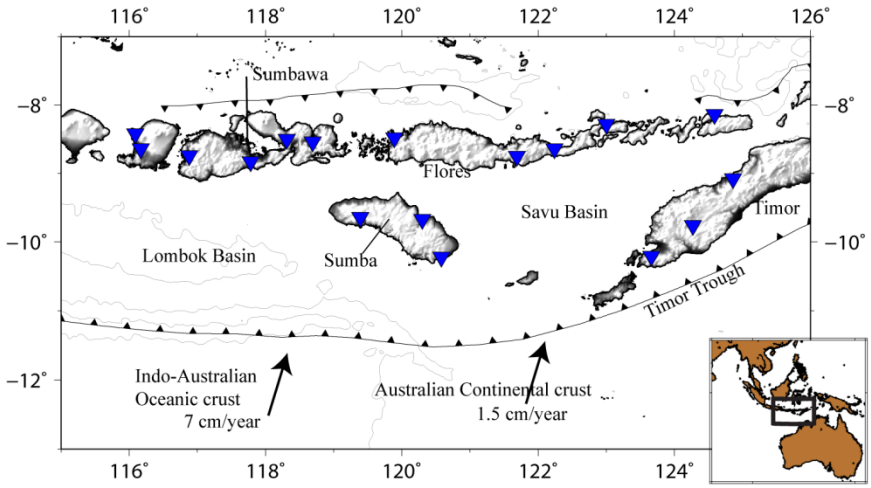

Figure 1. Map showing the tectonic setting of Sunda-Banda arc transition zone with the inverted blue triangles representing the seismic station used in this study.

Sunda-Banda arc transition zone (figure 1) is characterized by a change in tectonic setting from subduction of the Indo-Australian plate in west of Sumba to continent-island arc collision in east of Sumba [6]. The boundary of this transition zone is marked by the presence of Sumba Island, which is believed to be an isolated micro-continent block trapped in the forearc [7, 8]. However, the origin and evolution of Sumba Island is still debated [7]. The convergence rate at the west of Sumba is around 70 mm/yr [9] and decreases to ~15 mm/yr near the Timor Trough [10]. A previous seismic reflection study conducted in the west of Sumba observed that this region heavily faulted and fractured into 5-10 km wide blocks [11]. In the basin located east of Sumba, major structures are dominated by normal faults [12] and controlled by insertion of the promontory Australian continental crust beneath Banda arc. Furthermore, active volcanic islands mark the forearc boundary in the north of Sumba. A major structural discontinuity separating Sunda and Banda arc might exist between Sumbawa and Flores Islands as observed and proposed by geological and GPS studies [6, 13]. Timor Island marks the south boundary of the collision zone. This island is formed as a result of the collision between Australian plate and Banda arc [14]. The structure of the island is composed of complex group of rocks involving variety of deformed rocks including mafic and ultramafic rocks which mix together [15, 16].

2. Method

2.1. Shear-wave splitting

We implement splitting measurement using the automatic shear wave splitting algorithm, MFAST code [4]. This method is based on a grid search inversion of Silver and Chan [17] algorithm to compute splitting parameters (the fast polarization direction ϕ and delay time δt) for a given time window (figure 2). The method also incorporates cluster analysis introduced by Teanby *et al.* [18] to search the most stable measurement over a range of time windows. Multiple filters are used, and the

best filter is chosen based on the product of the signal-to-noise ratio and bandwidth. Uncertainties of the measurements are computed using F test for the selected time window by seeking the 95% confidence level for the optimum values of ϕ and δt. The selected splitting results are then graded from A to D reflecting good and bad results, based on the stability of the results obtained from the cluster analysis. Only the results with grades of at least B are selected for further processing. It is important to note that we only use the rays with incidence angles less than 35° to avoid contamination from the S-P conversion at the surface. The incidence angles are calculated using the TauP Toolkit [19] with the 1-D velocity models derived from receiver function study at each seismic station [20]. We observe that the models contain the low velocity layer at the near surface bending seismic rays into near-vertical propagation.

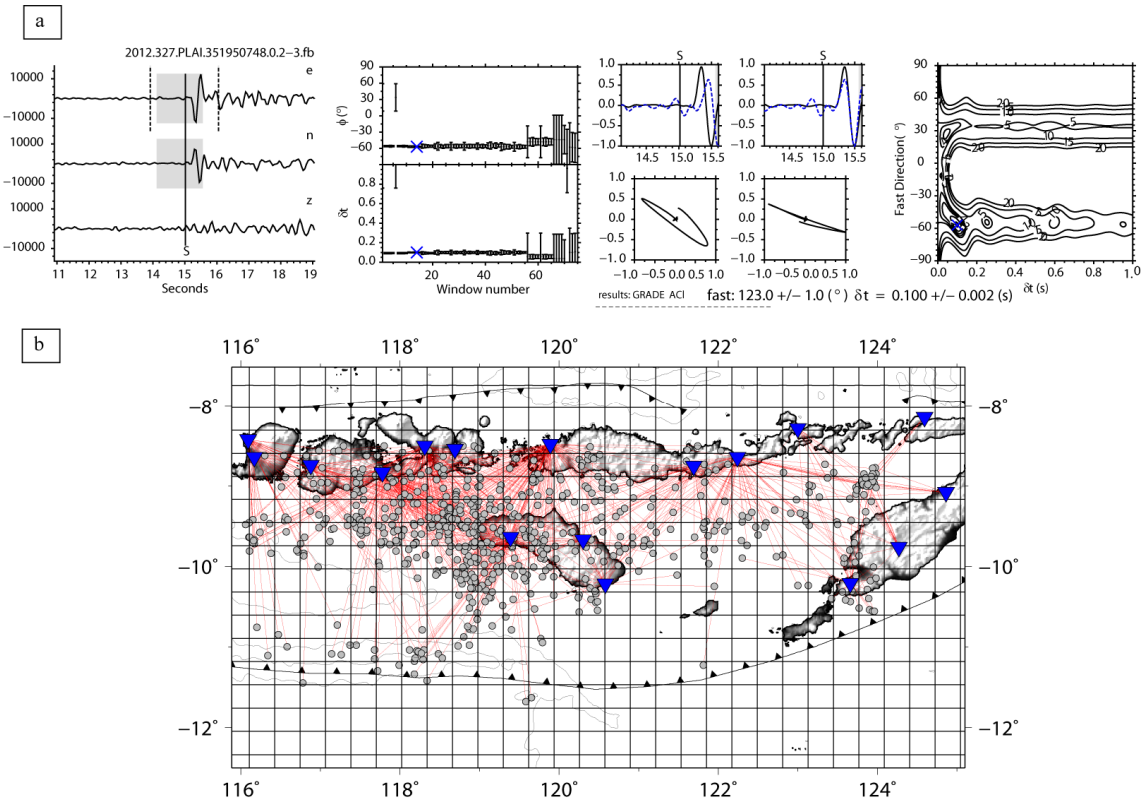

Figure 2. (a) An example of the splitting measurement obtained from MFAST. The left panel shows the three component seismogram with the S wave manual picking. The middle panels depict the cluster analysis to provide the best solution of splitting parameters, the waveforms and the particle motions of shear wave before and after correction for the splitting measurement, respectively. The right panel shows the contour diagram for the best solution denoted by the blue cross. (b) The earthquake epicenters (grey dots), raypaths (red lines) and grids used for the splitting analysis and inversion 2-D delay time tomography.

2.2. 2-D delay time (δt) tomography

To constrain the regions with low and high anisotropy, we employ 2-D delay time (δt) tomography using TESSA package developed by Johnson *et al.* [5]. The method measures the strength anisotropy in each of grid blocks assuming that the delay time (δt) is accumulated along the raypath. Thus, the relation between δt and path length L for each grid block can simply be written as:

$$\delta t_r = \sum_{b=1}^{n} S_b \times L_{rb}$$

where δt_r represents the estimated delay time of the ray r, S_b is the strength anisotropy for each grid block and L_{rb} is the path length of the ray r travelling within each of the n blocks. This equation can be solved using least square inversion to estimate the strength anisotropy. The solution satisfies the boundary condition in which the minimum value of strength anisotropy in each block is always greater than 0 km/s and the maximum values cannot exceed the maximum δt observed for a single block. Although this linear relationship reflects contrasts in the observed apparent δt rather than accurate values, the results still provide the first order approximation of heterogeneous anisotropic structure [5]. In this study, we use regular gridding with 32 km square blocks (figure 2).

3. Result and discussion

A large spatial variation in the splitting results obtained from the crustal events indicates complex anisotropic sources beneath the region [3] causing the interpretation difficult. Thus, to determine the average structure in the regions with low and high anisotropy and the most obvious trend of fast polarizations, we utilize 2-D delay time tomography and spatial averages of fast directions. Figure 3 depicts the δt tomography results using high-quality splitting parameters computed from 930 event-station pairs. We apply the ray coverage within the block, the checkerboard test results and the resolution maps above 5 (i.e. this value is chosen by considering that some blocks contain 8 passing rays) to define the limit of statistical significance illustrated by the white boundary lines in figure 3.

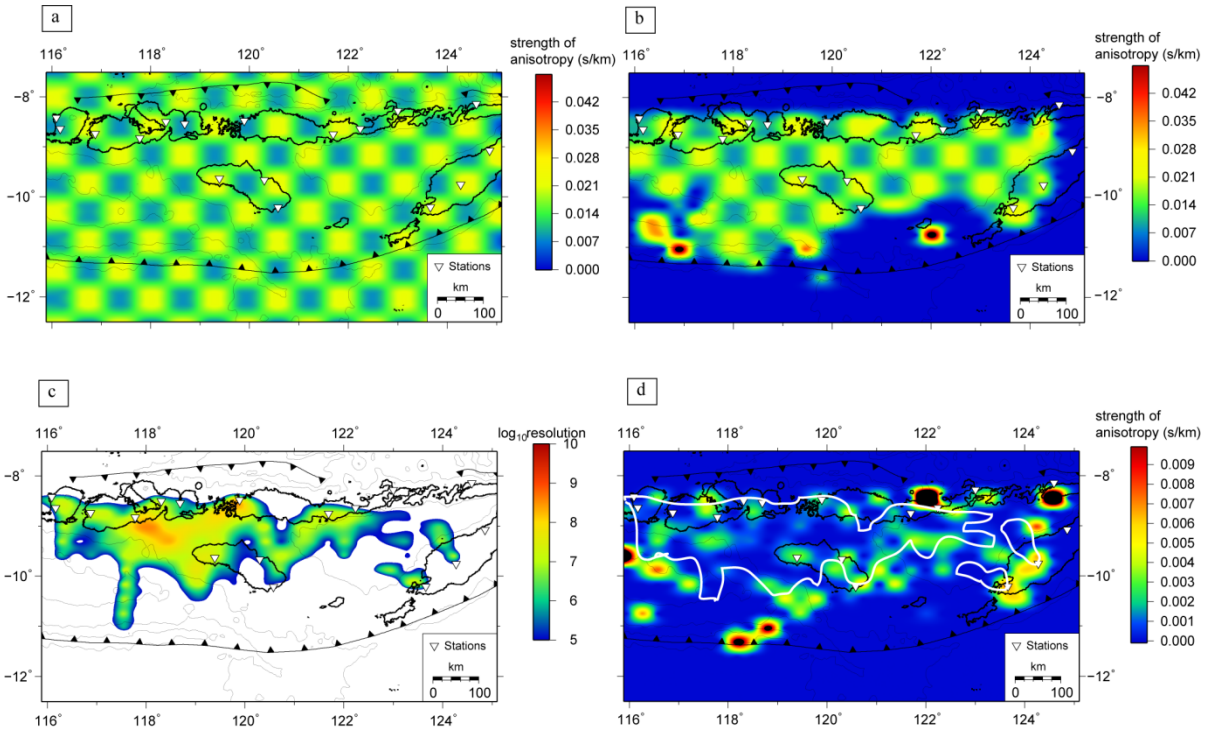

Figure 3. (a) Input for checkerboard test for 2-D delay time tomography. (b) Output for checkerboard test for 2-D delay time tomography using synthetic data created from the true rays passing through the checkerboard. (c) Resolution data inversion showing the limit of statistical significance computed from the model variance matrix [5]. (d) 2-D δt tomography using high-quality splitting parameters computed from 930 event-station pairs around the Sunda-Banda arc transition zone. The region with higher strength anisotropy is marked by warm colour (red to yellowish green), the weak anisotropic zone is denoted by blue colour. The white boundary line marks the region satisfying the resolution limit.

The inversion results indicate that the collision domain exhibits higher anisotropy (> 0.003 s/km), which may reflect the influence of the continent-arc collision. The high anisotropy found in this region coincides quite well with the region that experience crustal thickening (e.g. Savu Basin and Sumba) due to the insertion of Australian continental crust underneath southern part of the Banda arc. We observe possible high anisotropy beneath Lombok Basin. For the shallow depth, the area of Lombok Basin is characterized by more seismically active compared to the area in the east of Sumba Island [e.g. 21]. Previous seismic reflection studies show that that the crustal rocks beneath Lombok Basin are heavily fractured [e.g. 11, 22], suggesting that this area is actively deformed. The strong anisotropy is also observed in Timor Island. However, the island has very little earthquake activity, indicating stress induced anisotropy is not the only main source of anisotropy in this island. Thus, we suggest that the strong anisotropy in this island might correspond to the crustal fault zone or alignment of high anisotropic mineral such as gneisses, schist, and amphibolites as observed also by geophysical and geological studies [23, 24].

4. Conclusions

We apply 2-D shear wave splitting tomography to map lateral distribution of the possible sources of anisotropy in the Sunda-Banda transition zone. The result is in good agreement with structural features observed by previous geological and geophysical studies. For example, high anisotropy on Lombok Basin, Sumba, and Timor might correspond to the heavily fractured rocks associated to the active seismicity, fluid-filled crack related to the low-velocity zone due to insertion of continental crust, and the alignment of metamorphic and igneous rocks formed during later stages of continental-arc collision, respectively.

5. Acknowledgments

We acknowledge Indonesian Agency for Meteorology, Climatology, and Geophysics (BMKG) and GFZ Potsdam for their seismogram data. We are also grateful to Prof. Martha Savage and Jessica Johnson for providing softwares used in this study.

References

[1] Boness N L and Zoback M D 2004 *Geophys. Res. Lett.* **31** L15S17
[2] Boness N L and Zoback M D 2006 *Geology* **34** (10) 825-828
[3] Syuhada, Nugroho D H, Nanang T Puspito, Titi Anggono and Tedi Yudistira 2016 AIP Conference Proceedings **1719** 030042
[4] Savage M K, Wessel A, Teanby N A and Hurst A W 2010 *J. Geophys. Res.* **115** B12321
[5] Johnson J H, Savage M K and Townend J 2011 *J. geophys. Res.* **116** B12303
[6] Audley-Charles M G 1975 *Tectonophys* **26** 213-228
[7] Rutherford E, Burke K and Lytwyn J 2001 *J. Asian Earth Sci.* **19** 453– 479
[8] Abdullah C I, Rampnoux J P, Bellon H, Maury R C and Soeria-Atmadja R 2000 *J. Asian Earth Sci.* **18** 533-546
[9] Curray J R 1989 *Neth. J. Sea. Res.* **24** 131– 140
[10] Bock Y, Prawirodirdjo L, Genrich J F, Stevens C W, McCaffrey R, Subarya C, Puntodewo S S O and Calais E 2003 *J. geophys. Res.* **108** (B8) 2367
[11] Lueschen E, Mueller C, Kopp H, Engels M, Lutz R, Planert L, Shulgin A and Djajadihardja Y 2011 *Tectonophysics* **508** 1-4
[12] Rigg J W D and Hall R 2012 *Mar. Pet. Geol.* **32** 76-94
[13] Nugroho H, Harris R A, Amin W L and Bilal M 2009 *Tectonophys* **479** 52-65
[14] Harris R A and Audley Charles M G 1987 *Memoir Geological Society of China* **9** 45-61

[15] Barber A J, Audley-Charles M G and Carter D J 1977 *J. Geol. Soc. Australia* **24** 51–62
[16] Charlton T R 1989 *Aust. J. Earth. Sci.* **36** 263-274
[17] Silver P and Chan G 1991 *J. Geophys. Res.* **96** 16.429-16.454
[18] Teanby N A, Kendall J M and van der Baan M 2004 *Bull. Seismol. Soc. Am.* **94** 453–463
[19] Crotwell H P, Owens T J and Ristema J 1998 *Seismol. Res. Lett.* **70** 154-160
[20] Syuhada S, Hananto N D, Abdullah C I, Puspito N T, Anggono T and Yudistira T 2016 *Accepted Acta Geophysica*
[21] Ely K S and Sandiford M 2010 *Tectonophys.* **483** 112–124
[22] Van derWerff W 1996 *J. Southeast Asian Earth Sci.* **14** 331–349
[23] Karig D E, Barber A J, Charlton T R, Klemperer S E and Hussong D M 1987 *Geol. Soc. Am. Bull.* **93** 18–32
[24] Helmers J, Sopaheluwaken J, Tjokrosapoetro S, and Nila E S 1989 *Neth J Sea Res* **24** 357-371